Published in final edited form as:
Adv Mater. 2011 June 24; 23(24): H189–H194. doi:10.1002/adma.201100513.

Development of Cationic Polymer Coatings to Regulate Foreign Body Responses

Minglin Ma[1,4], **Wendy F. Liu**[1,4], **Paulina S. Hill**[1,2], **Kaitlin M. Bratlie**[1,4], **Daniel J. Siegwart**[1,2], **Justin Chin**[2], **Miri Park**[1,4], **Joao Guerreiro**[1], and **Daniel G. Anderson**[1,2,3,4,*]

[1]David H Koch Institute for Integrative Cancer Research, Massachusetts Institute of Technology, 77 Massachusetts Avenue, Cambridge, MA, 02139, USA

[2]Department of Chemical Engineering, Massachusetts Institute of Technology, 77 Massachusetts Avenue, Cambridge, MA, 02139, USA

[3]Division of Health Science Technology, Massachusetts Institute of Technology, 77 Massachusetts Avenue, Cambridge, MA, 02139, USA

[4]Department of Anesthesiology, Children Hospital Boston, 300 Longwood Ave, Boston, MA 02115, USA

Introduction

The biological responses to implanted biomaterials and medical devices play an important role in determining their long-term success.[1] Acute and chronic host response to foreign materials, and the formation of fibrotic tissue surrounding implants, can lead to compromised function, device failure and medical complications. [2,3,4] The foreign body response consists of a series of complex reactions involving various cell types, chemokines and cytokines. Recruitment of inflammatory cells such as neutrophils and macrophages to the implantation site is characteristic of the early response, i.e. acute inflammation, while fibrosis is typically associated with the later stages of chronic inflammation. Both physical and chemical properties of biomaterials influence the intensity and/or duration of the host response.[2] Numerous natural and synthetic materials have been used to fabricate coatings for implantable devices to mitigate their foreign body response.[5,6,7,8,9]

Mitigating the foreign body response is particularly important for successful cell encapsulation.[10] Delivery of encapsulated cells to target tissues holds great promise for treating a range of diseases including type I diabetes, many types of cancers, and neurodegenerative disorders such as Parkinson's.[11,12,13] One method for encapsulating cells is through the creation of a semi-permeable polyelectrolyte-complex capsule, which protects the encapsulated cells from immune system attack upon implantation while allowing for nutrient diffusion.[10] For example, in alginate-based microencapsulation systems, a polycation and the negatively charged alginate form a thin interpenetrating complex layer on the microcapsule surface that increases capsule stability and reduces permeability of inflammatory components, which may damage encapsulated cells.[14]

Poly-L-lysine (PLL) is the first polycation used for encapsulation of islet β-cells.[15] However, it has been reported that PLL induces a foreign body response, resulting in fibrotic capsules that eventually lead to islet necrosis. [16] Another example in which polycations are employed is in layer-by-layer (LBL) coatings, a versatile surface modification approach used in various biomedical applications such as anticoagulation and antimicrobial

*dgander@mit.edu; Tel.: +1 617 258 6843; fax: +1 617 258 8827.

applications.[17,18,19] The diversity of cationic polymers used in LBL coatings has been relatively limited. Typically used polycations include poly(allylamine hydrochloride) (PAH), poly(ethylene imine) (PEI), poly(diallylmethylammonium chloride) (PDAC), positively charged polypeptides and polysaccharide such as chitosan. To realize the full potential of LBL coatings and greatly accelerate the discovery of new applications and properties, more polycations with greater chemical diversity are desired.

Here, we describe our work generating a combinatorial library of novel cationic polymers, poly(β-amino alcohols) (PBAAs), and their evaluation as potential coatings for biomedical devices and cell encapsulation applications. Through an initial *in vitro* screening, we identified the polymer coatings that promoted or inhibited the activation of murine monocyte/macrophage cells by measuring the secretion of a pro-inflammatory cytokine, tumor necrosis factor α (TNF-α). The polymers that induced highest and lowest levels of TNF-α secretion were used to coat carboxylated polystyrene microparticles, which were subsequently injected subcutaneously into mice. Twenty-four hours after injection, significantly different levels of inflammatory cell recruitment into the implantation sites were observed through live animal imaging. Histological analysis of fibrosis around the particles 30 days after injection showed correlation with both the *in vitro* and *in vivo* imaging results, suggesting certain PBAA polymers are capable of mitigating the foreign body responses.

Poly(β – amino alcohols)

A library of 216 poly(β – amino alcohols) (PBAA) were made via step-growth polymerization of a diepoxide and a bis-secondary amine or a primary amine. Similar step growth polymerizations were used to make epoxy-based thermoplastics[20,21] and copoly(carbosiloxanes).[22] Figure 1 (a) shows the general structures of the monomers and polymers. These polymers have several advantages as potential coatings to regulate the foreign body response. First, they are hydrolytically stable and often hydrophilic due in part to abundant hydroxyl groups. Hydrophilicity has been recognized as a common characteristic of biomaterials with low protein adsorption or cell adhesion.[23,24] The non-biofouling properties of oligo(ethylene glycol)-terminated self-assembled monolayers (SAMs), [25] zwitterionic SAMs [26] and polymers [27] have been mainly attributed to their surface hydration. Second, synthesis of PBAAs is relatively simple and no solvents, high temperatures, or catalysts are required for production. Because of their general water-solubility and cationic nature, these polymers can be immobilized onto a wide range of negatively charged surfaces through electrostatic interactions. The mild coating conditions are particularly useful for coating medical devices that are sensitive to heat, UV light, or organic solvents. Lastly, the availability of a large number of monomers allows one to generate a diverse chemical library. A large number of chemically diverse polymers can be made through the variation of R_1, R_2 and R_3 in Figure 1 (a). The polymers were generally soluble in water or slightly acidic solutions with pH around 4 to 6. The polymers that were insoluble or formed hydrogels in water were eliminated for further study. Figure 1 (b) shows the chemical structures of the 6 epoxides and 36 amines chosen to make the polymers. 176 of these polymers were used for subsequent *in vitro* screening.

In Vitro Screening

We first sought to evaluate the effect of different PBAA coatings on monocyte/macrophage activation. To this end, we immobilized our library of PBAAs onto 96-well glass bottom plates. The surface of glass is generally hydrophilic and negatively charged under physiological conditions, and has been commonly used to immobilize polycations and build multilayer polyelectrolyte coatings. [28] Once immobilized, we measured the response of a murine monocyte/macrophage cell line to the coatings. Macrophages are one of the

dominant cell types that regulate the foreign body response. [29] The behavior of macrophages on surfaces with different charge densities, [30] topography[31, 32] and modulus[33] has been widely studied. It was found in particular that the surface chemistry[34,35,36,37] has direct influence on the macrophage-material interactions, although the chemical diversity of the surfaces that have been explored to date is limited.

Monocyte/macrophage response to different polymer coatings was assessed by measuring the TNF-α concentration in the cell culture media 18 hours after cell seeding. TNF-α is an important pro-inflammatory cytokine that plays a role in further recruitment and activation of inflammatory cells to injury sites.[38] The level of TNF-α secreted is an indicator of macrophage activation.[39,40] Figure 2 (a) shows the relative TNF-α concentration secreted by cells seeded on several of the coatings that were tested. Uncoated glass-bottom wells are used as controls. PLL and PAH, two typical commercially available cationic polymers, were used as additional references. Cells seeded on the least activating PBAAs showed a 10-fold lower level of TNF-α compared to cells seeded on the control, uncoated glass surface, and a 35-fold decrease compared to cells on the PLL coating. Scanning electron microscope (SEM) images revealed dramatic differences in cell morphology, as shown in Figure 2 (b) and (c). Cells that secreted high levels of TNF-α were more spread, whereas cells that secreted low levels of TNF-α remained rounded. (Supporting Information) The PBAAs that promoted macrophage activation all had similar acetal-functionalized side chains (amine monomers #22, #35, #36). Under acidic conditions, these acetal groups can be partially hydrolyzed into reactive aldehyde groups (Figure S3) which may promote the protein adsorption. The PBAAs that inhibited cell activation contained at least two tertiary amines per repeating unit (e.g. A10, A12, B20 and B30). The most inhibitory PBAA was A12, which has three tertiary amine groups in every repeating unit. While the mechanism by which the chemical functional groups affect macrophage activation is not clear at this stage, it is possible that the amount, composition and conformation of proteins adsorbed on the surface dictates the behavior of monocyte/macrophage cells.[41,42] Further studies show that the cell viability on all surfaces was essentially the same and comparable to cells seeded on control surfaces. (Supporting Information, Figure S4) Atomic Force Microscopy (AFM) studies revealed both the uncoated and coated surfaces were relatively smooth and the different levels of macrophage activation were not due to the topographical differences. (Figure S5) X-ray Photoelectron Spectroscopy (XPS) characterization and additional control experiments (Supporting Information, Figure S6) confirmed the stability of the coatings and the TNF-α secretion was mediated solely by coatings rather than solubilized coatings.

In Vivo Evaluation of Immune activation and Biocompatibility

To examine the inflammatory response to these novel materials *in vivo*, four different PBAAs that induced the highest (A35 and B35) and lowest (A12 and B12) levels of TNF-α secretion were chosen to coat 20 μm carboxylated polystyrene beads. Figure 3 (a) shows a SEM image of the beads with a schematic illustrating the coating. The size of the bead was selected to be large enough to limit phagocytosis [43] but small enough to allow easy injection under the skin. The chemical structures of A12 and B35 are shown in Figure 3 (b), and the configuration of the injections is shown by a schematic in Figure 3 (c). To measure the early foreign body responses to the injected beads, we examined the host response to beads coated with different PBAAs in live animals using fluorescent and bioluminescent imaging probes, Prosense®750 and luminol. Prosense is fluorescence sensor that measures the activity of Cathepsin B (and to a lesser extent Cathepsins K, L, and S).[44] The fluorescence signal correlates with the presence of neutrophils and monocyte/macrophages and can be used to assess the acute inflammatory response.[45] Figure 3 (d) shows the fluorescent images obtained using Prosense 24 hours after the particle injections. Quantification of the

fluorescent images show that A12 and B12 have lower signals than the A35 and B35, consistent with the trends observed *in vitro*.

Similar results were observed using luminol, a bioluminescent compound that reacts with reactive oxygen species (ROS) and emits blue luminescence.[46] It is known that during host responses to foreign bodies, neutrophils and macrophages release ROS, and therefore luminol has been used to measure the host response to implanted biomaterials.[47] The luminescent images obtained with luminol are shown in Figure 3 (e) and confirm again the correlation of the early foreign body responses with the *in vitro* screening results. Differences that exist in the quantification of the fluorescent and bioluminescent signals, most notably in the response to the control, can be attributed to the different cellular products measured. The uncoated polystyrene particles appear to elicit a more intense cathepsin response than ROS. This may be resultant of the different cell-type populations present at the implant site as well as their activation in response to the material. These differences illustrate the differences in dynamics of the foreign body response and necessitate the use of complementary techniques, such as cathepsin and ROS imaging. Further histological analysis of the skin tissues 30 days after injection (Supporting Information) showed that the least inflammatory coating A12 induced significantly less fibrosis compared with the most inflammatory coating B35 or the uncoated control.

In summary, we report the development of a new library of cationic polymers for biomedical applications. When used as surface coatings, these polymers elicited different levels of foreign body response, both *in vitro* and *in vivo*, depending on their chemical structures. The large chemical diversity of this class of materials allowed us to identify the polymer coatings that inhibited macrophage activation *in vitro*. Furthermore, these coatings reduced the recruitment of inflammatory cells 24 hours and fibrosis 30 days after subcutaneous implantation of PBAA coated carboxylated polystyrene microparticles. Using these polymers to form polyelectrolyte complex capsules for cell encapsulation is currently under investigation.

Experimental

Polymer Synthesis and Characterization

The monomers used to make the poly(β-amino alcohols) were purchased from Sigma-Aldrich (Milwaukee, WI), TCI America (Portland, OR) and Acros Organics (Fisher Scientific, Pittsburg, PA). All the epoxide and amine monomers used here are liquids at room temperature. The polymerizations took place in bulk at room temperature under vigorous stirring until solidification typically within 24 hours. Solvents such as dimethyl sulfoxide (DMSO) or dichloromethane could also be used but were not required for the reactions. To ensure all the polymers were terminated with amines, the molar ratio between amines and epoxides were controlled to be 1 to 1.2 in the polymerization. The polymers that were not soluble in water or form hydrogels with water were eliminated in the subsequent coatings. The molecular weights of representative PBAAs were determined using cationic columns in a Viscotek Gel Permeation Chromatography. A 2.7% acetic acid solution was used as the running solvent and the molecular weights were calculated relative to polyethyleneimine (PEI) standards. Depending on the specific structures of the monomers and reaction conditions, the typical weight averaged molecular weights (Mw) of the polymers ranged from 7,000 Da to 25,000 Da with polydispersity (PDI) of 1.5 to 2.5. (See Figure S2 in Supporting Information) The polymers were also characterized using a 400 MHz NMR Bruker Avance 400. The solvent was deuterated DMSO or chloroform. The ^{1}H NMR spectra of selected polymers exhibited clear peak broadening, typical of polymers. Two common chemical shift (ppm) ranges were around δ 2.2 - δ 2.8 (characteristic range of

H bonded to α C next to N) and δ 3.2 – δ 3.8 (characteristic range of H bonded to α C next to -OH). (See representative spectra in Figure S1.)

Surface Coatings and Characterization

PBAA solutions for coatings were made by dissolving the polymers in either DI water or slightly acidic solution at the concentration of 0.01 mol/L by repeating unit. The pH's of the solutions were adjusted to 4 to 7 using HCl solution and measured using a bench-top pH meter (Mettler Toledo). The solutions were coated on 96-well glass-bottom plates (Matrix Technologies Corp.) for *in vitro* screening. Each well was soaked with 150 μL different PBAA solutions for 1 hour. The wells were then washed thoroughly with DI water 5 times. The coatings were characterized with a Kratos Axis Ultra X-ray photoelectron spectrometer (XPS) (Kratos Analytical) with a monochromatized Al KR X-ray source. The takeoff angle relative to the sample substrate for this measurement was located at 90°. This means that the effective sampling depth is about a few nanometers. We seek only a qualitative confirmation of the surface coating at this stage, no attempt was made to obtain an accurate estimate of the actually surface coverage and coating thickness. The XPS signal from the nitrogen in the PBAA was used to confirm the surface coatings. Zeta potentials on glass surfaces were measured using a DelsaNanoC Particle Analyzer (Beckman Coulter) with a flat surface cell unit. The Zeta potential for uncoated glass surface was -73.5 mV; the surface coated with A12 and B35 had Zeta potentials of 24.8 mV and 23.4 mV, respectively. A Nanoscope IV, Dimension 3100 AFM (Digital Instruments, Santa Barbara, CA), in tapping mode, was used to image the surface structures. The images were analyzed using a software, NanoScope Analysis (Veeco Instruments Inc.) For *in vivo* tests, the PBAAs were coated on carboxylated polystyrene microspheres (20 μm diameter, PolySciences Inc.). The as-received microspheres were first washed with 70% ethanol once and subsequently DI water 6 times, and then incubated in 0.01 mol/L PBAA solutions for 2 hours for complete electrostatic bonding. The particles were washed again with DI water for 6 times and finally dispersed in PBS at a 10% (w/v) concentration for subsequent injections. The coatings on the particles and their stability were confirmed by measuring the zeta potentials of the particles before the coating, immediately after the coating and one month of storage in PBS after the coating. The zeta potential for the particles (0.0025% in DI water) determined by ZetaPALS (Brookhaven Instruments Corporation) was -38.1±4.9 mv before the coating, 35.1±5.5 mv after the A12 coating and 23.6±3.6 after 1 month storage.

In Vitro Screening

PBAA coated glass-bottom plates were first sterilized using 70% ethanol for 10 minutes and washed thoroughly with PBS. RAW 264.7 cells (ATCC) were cultured in DMEM supplemented with 10% fetal calf serum and penicillin/streptomycin (all from Invitrogen). Cells were seeded at a density of 150,000 cells/cm^2 on polymer-coated glass surfaces in serum containing media, incubated at 37°C for 18 h, and then analyzed for release of TNF-α and cell viability. To assess for TNF-α, cell culture supernatant was removed and analyzed by ELISA (R&D Systems) according to the manufacturer's instructions. Briefly, 96-well ELISA plates (BD Falcon) were coated with capture antibody overnight at 4°C. Plates were then washed three times with 0.01% Tween in PBS, blocked with 1% BSA in PBS, and then incubated with samples. After thorough washing, the captured TNF-α was detected using a detection antibody, HRP-conjugated streptavidin, and Ultra-TMB substrate (Pierce). The reaction was stopped with 0.16M sulfuric acid, and absorbance at 490nm was determined using a Spectramax plate reader (Molecular Devices). To assay for cell viability, cells were incubated with MTS ([3-(4,5-dimethylthiazol-2-yl)-5-(3-carboxymethoxyphenyl)-2-(4-sulfophenyl)-2H-tetrazolium) reagent (Promega) for 2 hours at 37°C, and absorbance at 490nm was measured. Visualization of live and dead cells was performed by staining with calcein and ethidium homodimer-1, respectively (Invitrogen). Fluorescence was visualized

on a Zeiss inverted microscope equipped with a 20X objective. Images were acquired using AxioVision software. All experiments were performed in triplicate and error bars indicate standard deviation from the mean. The cell morphology was further observed with a JEOL-6060SEM (JEOL Ltd., Japan) scanning electron microscope (SEM). The cells were first fixed using 4% formaldehyde solution for 30 minutes after being washed with PBS twice. The fixed samples were then rinsed with DI water and dehydrated using a sequence of progressively more concentrated ethanol solutions (30%, 50%, 70%, 90% and 100%). After a few hours of air-drying, the cells were sputter-coated with a 2-3 nm layer of gold for imaging by use of a Desk II cold sputter/etch unit (Denton Vacuum LLC). Quantification of cell morphology was obtained by analyzing the maximum diameter of each cell (n>75 per coating) using Sigma Scan Pro digital imaging software. The average maximum diameter values were expressed as a percentage of the uncoated control.

In Vivo Imaging

PBAA coated microparticles were injected subcutaneously in an array format on the backs of immunocompetent hairless mice (SKH1, Charles River Laboratories, Wilmington, MA). The mice were maintained at the animal facilities of Massachusetts Institute of Technology, accredited by the American Association of Laboratory Animal care, and were housed under standard conditions with a 12-hour light/dark cycle. Both water and food were provided *ad libitum*. The animal protocol was approved by the Committee on Animal Care at Massachusetts Institute of Technology prior to initiation of the research. Each injection contained 100 μL 10% (w/v) particle suspension in PBS. The mice were anesthetized with isoflurane inhalation at a concentration of 1-4% isoflurane/balance O_2 and their backs were scrubbed with alcohol patches before the injections. *In vivo* fluorescence and bioluminescence imaging was performed by using an IVIS imaging system (IVIS Spectrum, Caliper Life Sciences, Hopkinton, MA) and the images were analyzed with Living Image acquisition and analysis software (Caliper Life Sciences, Hopkinton, MA). The Prosense®750 (VisEn Medical, Woburn, MA) was injected through the tail vein (i.v.) at a dose of 100 μL per mouse 24 hours before imaging. Luminol (Aldrich) was injected intraperitoneally (i.p.) 20 minutes before imaging at a dose of 5mg per mouse. The mice were anesthetized with isoflurane for the i.p. injection and imaging.

Histological Analysis

Mice were euthanized via CO_2 asphyxiation. Skin samples containing the injected microparticles were fixed in AccuStain (Aldrich), embedded in paraffin, sectioned and stained with Masson Trichrome based on standard procedures. The histology slides were then observed using a Zeiss inverted microscope. Images at both 5X and 20X were taken to view the global fibrosis around the entire implantation site as well as local fibrosis around individual particles. To evaluate the fibrosis around individual particles, digital image analysis of 20X images was performed using Sigma Scan Pro 5.0 (Aspire Software International, Ashburn, VA) Using a color threshold, the percentage of collagenous (blue) material for each sample as a percentage of the total implanted microparticle area was quantified. The values were presented as the mean ± standard deviation of the mean. Comparisons of different samples were performed using the Student's unpaired two-tailed t-test. $p < 0.05$ was considered statistically significant.

Supplementary Material

Refer to Web version on PubMed Central for supplementary material.

Acknowledgments

This research was supported by the Juvenile Diabetes Research Foundation under grant 17-2007-1063. K.B. is grateful to the support from the National Institutes of Health postdoctoral fellowship F32 EB011580-01. We are grateful to Dr. Christopher Levins, Dr. Arturo Vegas and Nisarg Shah for the discussions, and Mr. Chakib Boussahmain for assistance with histology.

References

1. Langer R. Adv Mater. 2009; 21:3235. [PubMed: 20882493]
2. Anderson JM. Annu Rev Mater Res. 2001; 31:81.
3. Novak MT, Bryers JD, Reichert WM. Biomaterials. 2009; 30:1989. [PubMed: 19185345]
4. Williams DF. Biomaterials. 2008; 29:2941. [PubMed: 18440630]
5. Ratner BD, Bryant SJ. Annu Rev Biomed Eng. 2004; 6:41. [PubMed: 15255762]
6. Ward WK. J Diabetes Sci Technol. 2008; 2:768. [PubMed: 19885259]
7. Onuki Y, Bhardwaj U, Papadimitrakopoulos F, Burgess DJ. J Diabetes Sci Technol. 2008; 2:1003. [PubMed: 19885290]
8. DeFife KM, Shive MS, Hagen KM, Clapper DL, Anderson JM. J Biomed Mater Res. 1999; 44:298. [PubMed: 10397932]
9. Goreish HH, Lewis AL, Rose S, Lloyd AW. J Biomed Mater Res. 2004; 68A:1.
10. Chang TMS. Nature Reviews Drug Discovery. 2005; 4:221.
11. Calafiore R, et al. Diabetes Care. 2006; 29:137. [PubMed: 16373911]
12. Joki T, et al. Nature Biotech. 2001; 19:35.
13. Kishima H, Poyot T, Bloch J, Dauguet J, Condé F, Dollé F, Hinnen F, Pralong W, Palfi S, Déglon N, Aebischer P, Hantraye P. Neurobiol Dis. 2004; 16:428. [PubMed: 15193299]
14. Strand BL, Morch YA, Espevik T, Skjak-Brak G. Biotechnol Bioeng. 2003; 82:386. [PubMed: 12632394]
15. Lim F, Sun AM. Science. 1980; 210:908. [PubMed: 6776628]
16. Orive G, et al. Nature Medicine. 2003; 9:104.
17. Boudou T, Crouzier T, Ren K, Blin G, Picart C. Adv Mater. 2010; 22:441. [PubMed: 20217734]
18. Decher G. Science. 1997; 277:1232.
19. Hammond PT. Adv Mater. 2004; 16:1271.
20. White JE, Silvis HC, Winkler MS, Glass TW, Kirkpatrick DE. Adv Mater. 2000; 12:1791.
21. White JE, Earls J, Sherman JW, Lopez LC, Dettloff ML. Polymer. 2007; 48:3990.
22. Grunlan MA, Lee NS, Weber WP. Polymer. 2004; 45:2517.
23. Ostuni E, Chapman RG, Holmlin RE, Takayama S, Whitesides GM. Langmuir. 2001; 17:5605.
24. Peppas NA, Hilt JZ, Khademhosseini A, Langer R. Adv Mater. 2006; 18:1345.
25. Harder P, Grunze M, Dahint R, Whitesides GM, Laibinis PE. J Phys Chem B. 1998; 102:426.
26. Holmlin RE, Chen X, Chapman RG, Takayama S, Whitesides GM. Langmuir. 2001; 17:2841.
27. Jiang S, Cao Z. Adv Mater. 2010; 22:920. [PubMed: 20217815]
28. Mendelsohn JD, Yang SY, Hiller JA, Hochbaum AI, Rubner MF. Biomacromolecules. 2003; 4:96. [PubMed: 12523853]
29. Anderson JM. Cardiovasc Pathol. 1993; 2:S33.
30. Hunt JA, Flanagan BF, McLaughlin PJ, Strickland I, Williams DF. J Biomed Mater Res. 1996; 31:139. [PubMed: 8731158]
31. Refai AK, Textor M, Brunette DM, Waterfield JD. J Biomed Mater Res. 2004; 70A:194.
32. Paul NE, et al. Biomaterials. 2008; 29:4056. [PubMed: 18667233]
33. Irwin EF, Saha K, Rosenbluth M, Gamble LJ, Castner DG, Healy KE. J Biomater Sci Polymer Edn. 2008; 19:1363.
34. Brodbeck WG, Nakayama Y, Matsuda T, Colton E, Ziats NP, Anderson JM. Cytokine. 2002; 18:311. [PubMed: 12160519]

35. Schutte RJ, Parisi-Amon A, Reichert WM. J Biomed Mater Res. 2009; 88A:128.
36. Kamath S, Bhattacharyya D, Padukudru C, Timmons RB, Tang L. J Biomed Mater Res. 2008; 86A:617.
37. Collier TO, Anderson JM, Brodbeck WG, Barber T, Healy KE. J Biomed Mater Res. 2004; 69A: 644.
38. Brodbeck WG, Voskerician G, Ziats NP, Nakayama Y, Matsuda T, Anderson JM. J Biomed Mater Res A. 2003; 64:320. [PubMed: 12522819]
39. Anderson, JM. Inflmmation, wound healing, and the foreign-body response. In: Ratner, BD.; Hoffman, AS.; Schoen, FJ.; Lemons, JE., editors. Biomaterials Science An introduction to materials in medicine. San Diego, CA: Elsevier; 2004. p. 296-304.
40. Panilaitis B, Altman GH, Chen J, Jin HJ, Karageorgious V, Kaplan DL. Biomaterials. 2003; 24:3079. [PubMed: 12895580]
41. Tamada Y, Ikada Y. J Colloid Interf Sci. 1993; 155:334.
42. Mei Y, et al. Nature Mater. 2010; 9:768. [PubMed: 20729850]
43. Champion JA, Walker A, Mitragotri S. Pharm Res. 2008; 25:1815. [PubMed: 18373181]
44. Nahrendorf M, Sosnovik DE, Waterman P, Swirski FK, Pande AN, Aikawa E, Figueiredo JL, Pittet MJ, Weissleder R. Circ Res. 2007; 100:1218. [PubMed: 17379832]
45. Bratlie KM, Dang TT, Lyle S, Nahrendorf M, Weissleder R, Langer R, Anderson DG. PLoS ONE. 2010; 5:e10032. [PubMed: 20386609]
46. Gross S, Gammon ST, Moss BL, Rauch D, Harding J, Heinecke JW, Ratner L, Piwnica-Worms D. Nature Medicine. 2009; 15:455.
47. Liu WF, Ma M, Bratlie KM, Dang TT, Langer R, Anderson DG. Biomaterials. 2011; 32:1796. [PubMed: 21146868]

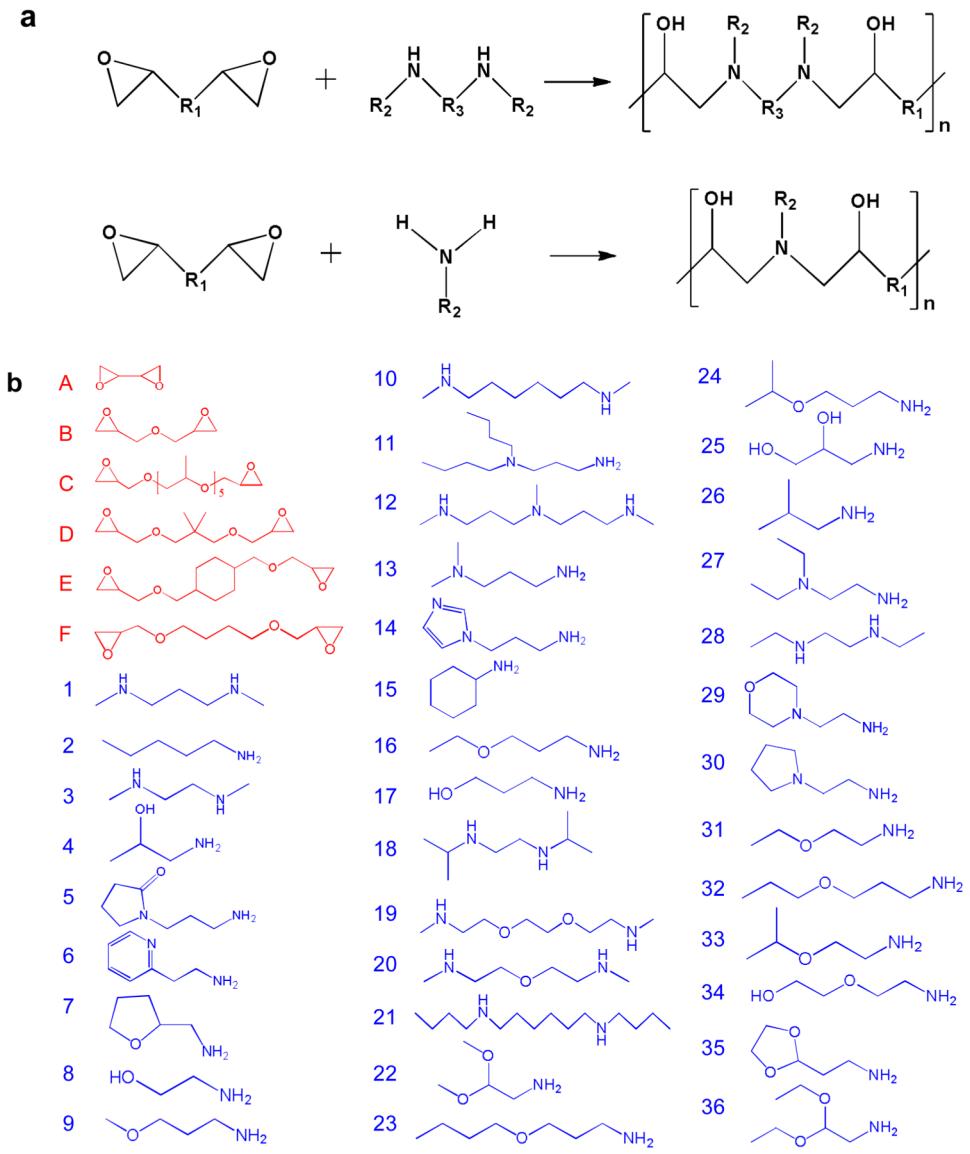

Figure 1.
Synthesis of a new library of poly(β-amino alcohols). (a) General scheme of step-growth polymerization. (b) The epoxide (A-F) and amine (1-36) monomers used to make PBAAs.

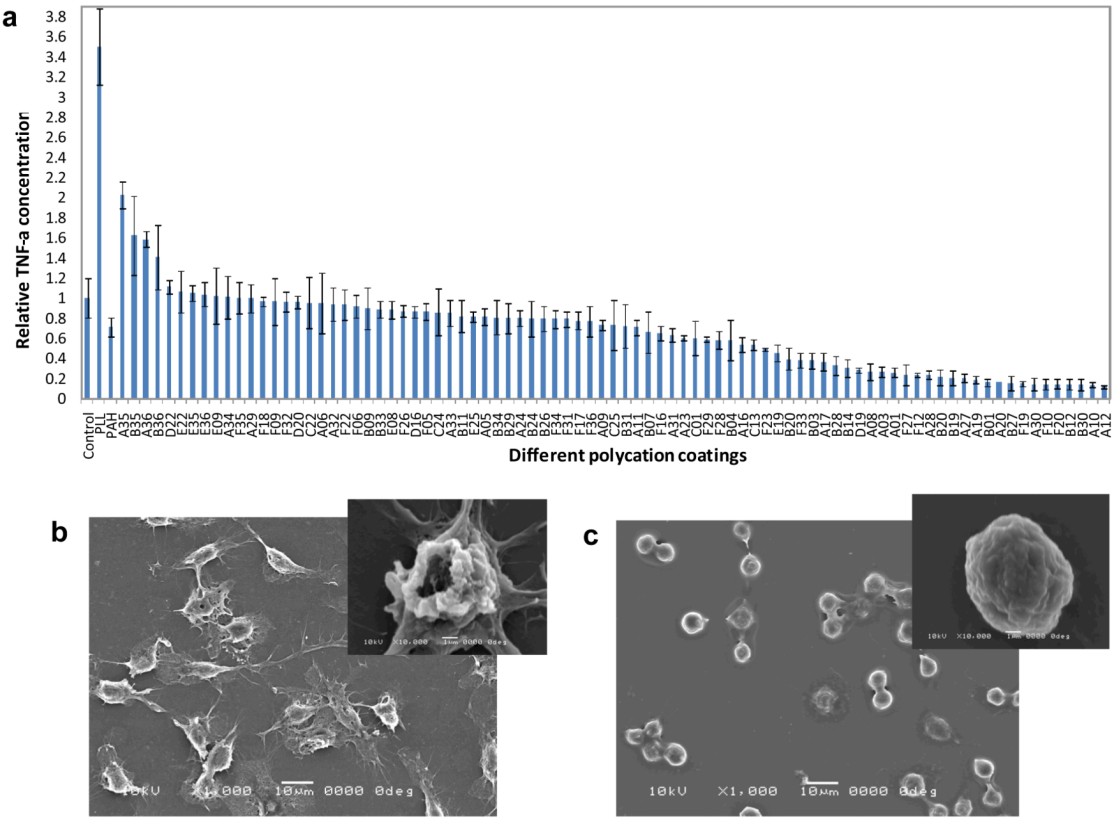

Figure 2.

In vitro screening of PBAAs for biocompatible coatings using monocyte/macrophage cells. (a) The dependence of TNF-α concentration on surface chemistry. The control is the uncoated glass surface. (b) and (c), SEM images showing the morphological differences of the cells between uncoated surface (b) and B20 coated surface (c). The insets are the morphologies of single cells.

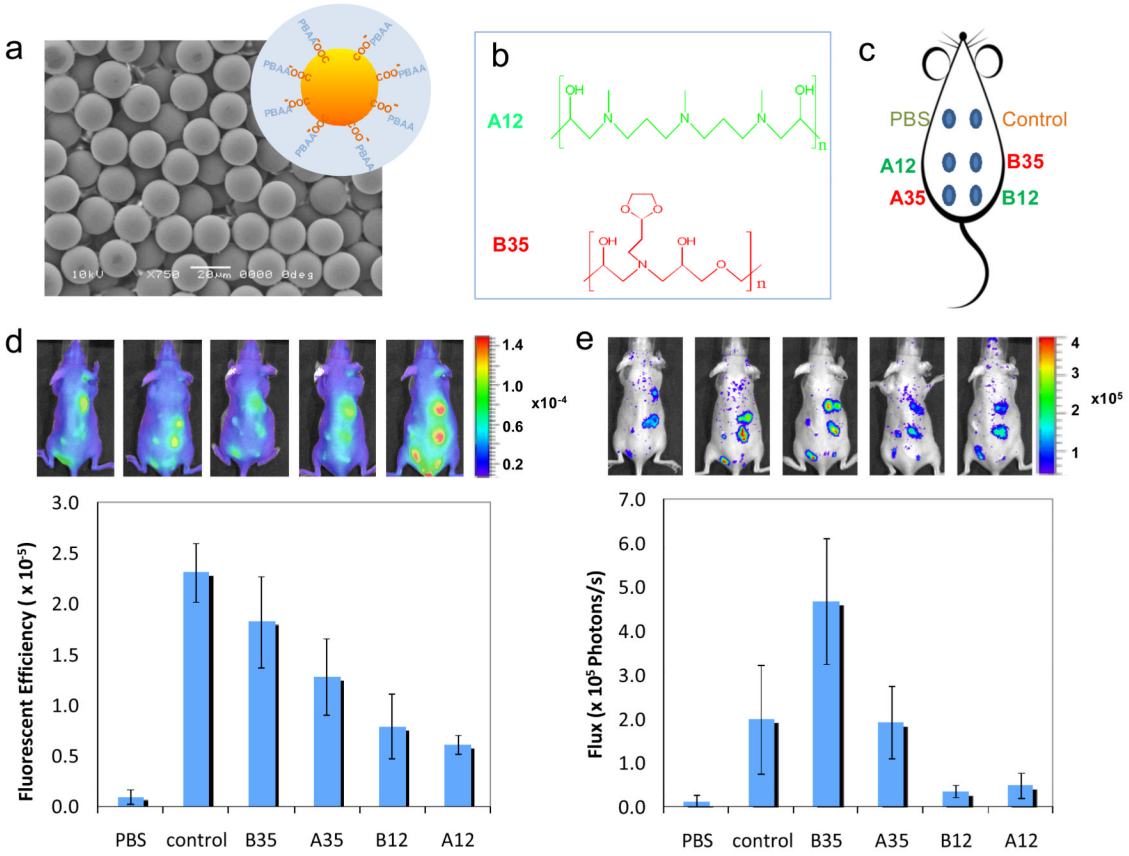

Figure 3.

Imaging of live animals with subcutaneously-injected PBAA-coated microparticles. (a) SEM image of carboxylated polystyrene beads used as the substrate for PBAA coatings. The inset is the schematic of the PBAA coating on the particles (not to scale). (b) Chemical structures of A12 and B35, which inhibits and promotes the activation of monocyte/macrophage cells in vitro, respectively. (c) The configuration of 6 injections on the back of a mouse. (d) Fluorescent images of mice (5 replicates) 24 hours after injections using Prosense as the probe and quantitative results from the image analysis. (e) Luminescent image of the same 5 mice using Luminol as the probe and quantitative results.